Closed-form solutions to the effective properties of fibrous magnetoelectric composites and their applications

L. P. Liu [a,b], H.-Y. Kuo [c,*]

[a] *Department of Mechanical and Aerospace Engineering, Rutgers University, NJ 08854, U.S.A.*

[b] *Department of Mathematics, Rutgers University, NJ 08854, U.S.A.*

[c] *Department of Civil Engineering, National Chiao Tung University, Hsinchu 300, Taiwan, R.O.C.*

Abstract

Magnetoelectric coupling is of interest for a variety of applications, but is weak in natural materials. Strain-coupled fibrous composites of piezoelectric and piezomagnetic materials are an attractive way of obtaining enhanced effective magnetoelectricity. This paper studies the effective magnetoelectric behaviors of two-phase multiferroic composites with periodic array of inhomogeneities. For a class of microstructures called periodic E-inclusions, we obtain a rigorous closed-form formula of the effective magnetoelectric coupling coefficient in terms of the shape matrix and volume fraction of the periodic E-inclusion. Based on the closed-form formula, we find the optimal volume fractions of the fiber phase for maximum magnetoelectric coupling and correlate the maximum magnetoelectric coupling with the material properties of the constituent phases. Based on these results, useful design principles are proposed for engineering magnetoelectric composites.

Key words: magnetoelectricity, periodic composites, E-inclusion, generalized anti-plane shear deformation, optimal design

* Corresponding author.
Email address: hykuo@mail.nctu.edu.tw (H.-Y. Kuo).

1 Introduction

Magnetoelectricity (ME) refers to the magnetization induced by an electric field, or conversely the polarization induced by a magnetic field. The ME effect has many important technological applications, ranging from large-area sensitive detection of magnetic fields (Fiebig, 2005), magnetoelectric memory cells (Kumar et al., 2009), and to electrically controlled microwave phase shifters (Bichurin et al., 2002). However, the ME coupling coefficient is barely noticeable for most single-phase materials in spite of recent discovery of gigantic magnetoelectric effects in $TbMnO_3$ at cryogenic temperature (Kimura et al., 2003). Therefore various researchers have turned to composites or nano-structured materials (Zheng et al., 2004; Fennie, 2008), as explained in recent reviews of Eerenstein et al. (2006) and Nan et al. (2008). The "product property" causes the ME effect in composites of piezoelectric (PE) and piezomagnetic (PM) materials: an applied electric field generates a strain in the piezoelectric material which in turn induces a strain in the piezomagnetic material, resulting in a magnetization.

The promise of applications, and the indirect coupling through strain have also made ME composites the topic of a number of theoretical and experimental investigations (Nan et al., 2008; Zheng et al., 2004). The estimates of the effective properties of ME composites of non-dilute volume fractions are usually obtained by mean-field-type models (Nan, 1994; Srinivas and Li, 2005). Exact relations in a ME composite with composite cylinder assemblage microgeometry were derived by Benveniste (1995), and the analysis for local fields is available for simple microstructures such as a single ellipsoidal inclusion (Huang and Kuo, 1997; Li and Dunn, 1998a), periodic array of circular/elliptic fibrous ME composites (Kuo, 2011; Kuo and Pan, 2011) and laminates (Kuo et al., 2010), etc. Numerical methods based on the finite element method have also been developed to address ME composites for general microstructures (Liu et al., 2004; Lee et al., 2005), while homogenization methods were proposed by Aboudi (2001) and Camacho-Montes et al. (2009).

In this paper we consider two-phase composites of piezoelectric (PE) materials and piezomagnetic (PM) materials and seek closed-form predictions of their effective properties by generalizing the uniformity property of ellipsoids to other geometries, namely, periodic E-inclusions. In the classic work of Eshelby (1957, 1961), he discovered that any uniform eigenstress on an ellipsoidal inclusion induces uniform strain on the inclusion in an infinite homogeneous medium. This remarkable *uniformity* property of ellipsoids allows for rigorous closed-form solutions to inhomogeneous problems by the so-called equivalent inclusion method, which has been used to develop many important materials models concerning composites, phase transformations, dislocations and cracks, etc. (Mura, 1987). However, since two or more ellipsoids do not enjoy the

uniformity property, analysis based on Eshelby's solution and the equivalent inclusion method cannot account for the interactions between inhomogeneities, e.g., composites with non-dilute inhomogeneities. To overcome this limitation, mean-field-type Mori-Tanaka models have been developed to address multiferroic composites by Li and Dunn (1998a,b), Huang (1998), Li (2000), Wu and Huang (2000) and Srinivas et al. (2006). In addition, a phase-field method based on a generalized Eshelby's equivalency principle is proposed for arbitrary microstructures (Ni et al., 2010).

Following the work of Eshelby (1957), Liu et al. (2007; 2008) have recently found a periodic generalization of ellipsoids called *periodic E-inclusions* (also called Vigdergauz microstructures in two dimensions). Periodic E-inclusions share partially the uniformity property of ellipsoids: a uniform dilatational eigenstress on the periodic E-inclusions induces uniform strain on the periodic E-inclusions for isotropic materials. Since it is not the ellipsoid *per se* but its *uniformity* property that is being used in the classic analysis based on Eshelby's solution, we extend the argument of equivalent inclusion method for ellipsoidal inclusions to periodic E-inclusions and achieve explicit closed-form solutions to the effective properties of the composites and local fields. This strategy has been used to predict the effective properties of conductive composites (Liu, 2009) and elastic composites (Liu et al., 2008). Here we present the detailed calculations for composites of PE and PM materials. Aiming to improve the magnetoelectric (ME) coupling of the composite, we further study how the effective ME voltage coefficient, the figure of merit of ME materials, depends on the volume fraction, the topology of microstructures and the material properties of constituent phases. In particular, we find the optimal volume fraction of the fiber phase for maximum effective voltage coefficient and draw a few useful design principles, which are summarized in Section 5.

The paper is organized as follows. In Section 2 we formulate the governing equation for a periodic piezoelectric-piezomagnetic composite and define the effective properties of the composite. In Section 3 we introduce the periodic E-inclusion and derive the closed-form formula of the effective properties of a composite with a periodic E-inclusion microstructure. In Section 4 we study how the magnetoelectric voltage coefficient depends on volume fractions of the fiber phase and material properties of constituent phases. Finally we summarize a few useful design principles in Section 5.

2 Problem statement

We consider a composite consisting of a periodic array of parallel and separated prismatic cylinders as sketched in Fig. 1. The cylinders and the matrix are made of distinct phases: transversely isotropic piezoelectric or piezomagnetic

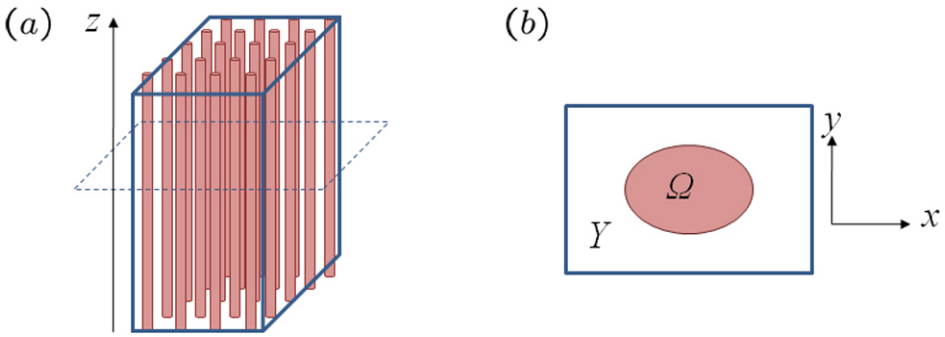

Fig. 1. Configuration of the fibrous composite: (a) the overall composite and (b) a unit cell in the xy-plane with Ω being one phase and $Y \setminus \Omega$ being the other phase.

materials. A Cartesian coordinate system is introduced with the xy-axes in the plane of the cross-section and z-axis along the axes of the cylinders. Let Y be a unit cell in the xy-plane and $\Omega \subset Y$ denote the cross-section of the cylinder in this unit cell.

Assume that the composite be subjected to anti-plane shear strains $\overline{\varepsilon}_{zx}$, $\overline{\varepsilon}_{zy}$, in-plane electric fields $\overline{E}_x$, $\overline{E}_y$ and magnetic fields $\overline{H}_x$, $\overline{H}_y$ at infinity. It can be shown that the composite is in a state of generalized anti-plane shear deformation and can be described by (Benveniste, 1995)

$$\begin{aligned} &u_x = u_y = 0,\ u_z = w(x,y), \\ &\varphi = \varphi\,(x,y)\,,\ \psi = \psi\,(x,y)\,, \end{aligned} \tag{1}$$

where u_x, u_y, u_z are the elastic displacements along the x- , y-, and z- axis, and φ and ψ are, respectively, the electric and magnetic potentials.

The general constitutive law of the rth phase for the non-vanishing field quantities can be written in a compact form as

$$\mathbf{\Sigma}^{(r)} = \mathbf{L}^{(r)}\mathbf{Z}^{(r)}, \qquad \mathbf{L}^{(r)} = \begin{cases} \mathbf{L}^{(i)} & \text{if } \mathbf{x} \in \Omega, \\ \mathbf{L}^{(m)} & \text{if } \mathbf{x} \in Y \backslash \Omega, \end{cases} \tag{2}$$

where for ease of the terminology, $r =$ "m" ($r =$ "i") refers to the matrix (inclusion) phase,

$$\mathbf{\Sigma}^{(r)} = \begin{pmatrix} \sigma_{zx},\ \sigma_{zy} \\ D_x,\ D_y \\ B_x,\ B_y \end{pmatrix}^{(r)}, \ \mathbf{Z}^{(r)} = \begin{pmatrix} \varepsilon_{zx},\ \ \varepsilon_{zy} \\ -E_x,\ -E_y \\ -H_x,\ -H_y \end{pmatrix}^{(r)} = \begin{pmatrix} \partial_x w,\ \partial_y w \\ \partial_x \varphi,\ \partial_y \varphi \\ \partial_x \psi,\ \partial_y \psi \end{pmatrix}^{(r)}, \tag{3}$$

and $(p, q = 1, 2, 3;\ i, j = 1, 2 \text{ or } x, y)$

$$L_{piqj}^{(r)} = A_{pq}^{(r)} \delta_{ij}, \qquad A_{pq}^{(r)} = \begin{pmatrix} C_{44} & e_{15} & q_{15} \\ e_{15} & -\kappa_{11} & -\lambda_{11} \\ q_{15} & -\lambda_{11} & -\mu_{11} \end{pmatrix}^{(r)} . \tag{4}$$

In Eq. (3) and Eq. (4), σ_{zj}, D_j, B_j, ε_{zj}, E_j, and H_j $(j = x, y)$ are the stress, electric displacement, magnetic flux, strain, electric field, and the magnetic field, respectively. The materials constants C_{44}, κ_{11}, μ_{11} and λ_{11} are the elastic modulus, dielectric permittivity, magnetic permeability and ME coefficient, while e_{15} and q_{15} are the piezoelectric and piezomagnetic constants. The shear strains ε_{zx} and ε_{zy}, in-plane electric fields E_x, E_y, and in-plane magnetic fields H_x and H_y are given by the gradient of the elastic anti-plane displacement w, electric potential φ, and magnetic potential ψ.

We assume the microstructure of the composite is periodic and the composite is subject to a macroscopic average applied field

$$\mathbf{F} = \begin{pmatrix} \overline{\varepsilon}_{zx} & \overline{\varepsilon}_{zy} \\ -\overline{E}_x & -\overline{E}_y \\ -\overline{H}_x, & -\overline{H}_y \end{pmatrix}.$$

From the homogenization theory (Milton, 2002), the microscopic local fields and effective properties are determined by the unit cell problem

$$\begin{cases} \nabla \cdot [\mathbf{L}(\mathbf{x})(\nabla \mathbf{u} + \mathbf{F})] = 0 & \text{on } Y, \\ \text{periodic boundary conditions on } \partial Y, \end{cases} \tag{5}$$

where $\mathbf{u} = [w, \varphi, \psi]^T$ is the column vector field formed by the displacement, electric and magnetic potentials, and the tensor $\mathbf{L}(\mathbf{x})$ takes the value of $\mathbf{L}^{(i)}$ if $\mathbf{x} \in \Omega$ and $\mathbf{L}^{(m)}$ if $\mathbf{x} \in Y \setminus \Omega$. Further, the effective properties of the composite, denoted by the tensor $\mathbf{L}^e$, are given by

$$\overline{\mathbf{\Sigma}} = \mathbf{L}^e \mathbf{F}, \qquad \overline{\mathbf{\Sigma}} = \frac{1}{|Y|} \int_Y \mathbf{\Sigma}(\mathbf{x})\, d\mathbf{x}, \quad \mathbf{\Sigma}(\mathbf{x}) = \mathbf{L}(\mathbf{x})(\nabla \mathbf{u} + \mathbf{F}), \tag{6}$$

where $|\cdot|$ denotes the area of a domain. From Eq. (6), we can alternately define the effective tensor $\mathbf{L}^e$ by the quadratic form

$$\mathbf{F}\cdot\mathbf{L}^{e}\mathbf{F}=\frac{1}{|Y|}\int_{Y}\mathbf{F}\cdot\mathbf{L}\left(\mathbf{x}\right)\left(\nabla\mathbf{u}+\mathbf{F}\right)d\mathbf{x}. \tag{7}$$

3 The closed-form solutions

A closed-form analytical solution to Eq. (5) is not anticipated for general microstructure. Nevertheless, for periodic E-inclusions we solve Eq. (5) by the well-known Eshelby equivalent inclusion method. Below we first present a brief description of periodic E-inclusions and then solution to Eq. (5).

3.1 Periodic E-inclusions: existence and property

Motivated by the broad applications of Eshelby's solutions in a variety of materials models, Liu, James and Leo (2007; 2008) generalized the geometric shape of ellipsoids according to their *uniformity* property in the context of Newtonian potential problem, i.e., the Newtonian potential $\phi : I\!R^n \to I\!R$ ($n \geq 2$ is the dimension of space) induced by a homogeneous ellipsoid Ω satisfies the *overdetermined* problem:

$$\begin{cases} \Delta\phi=-\chi_{\Omega} & \text{on } I\!R^{n}, \\ \nabla\nabla\phi=-\mathbf{Q} & \text{on } \Omega, \\ |\nabla\phi|\to 0 & \text{as } |\mathbf{x}|\to+\infty, \end{cases} \tag{8}$$

where χ_Ω is the characteristic function of Ω, equal to one on Ω and vanishing otherwise, and $\mathbf{Q}$ is a nonnegative symmetric $n\times n$ matrix with $\mathrm{Tr}(\mathbf{Q})=1$. In analogy with Eq. (8), a periodic E-inclusion in a unit cell $Y\subset I\!R^n$ is defined as a domain Ω such that the solution to the potential problem(Liu et al., 2008)

$$\begin{cases} \nabla^{2}\phi=f-\chi_{\Omega} & \text{on } Y, \\ \text{periodic boundary conditions} & \text{on } \partial Y, \end{cases} \tag{9}$$

satisfies the overdetermined condition

$$\nabla\nabla\phi=-(1-f)\mathbf{Q} \qquad \text{on } \Omega, \tag{10}$$

where $f=|\Omega|/|Y|$ is the volume fraction of the inclusion. The terminology "E-inclusion" arises from the associations with "Eshelby", "Ellipsoid" and

"Extremal" properties of such geometries.

The overdetermined condition Eq. (10) places strong restrictions on the domain Ω. The existence of periodic E-inclusions can be established by considering a simple *variational inequality* (Friedman, 1982):

$$G[\phi] = \min_{u \in \mathbb{W}} \Big\{ G[u] := \int_Y [\tfrac{1}{2}|\nabla u| + fu] \Big\}, \tag{11}$$

where the admissible potential $\mathbb{W} := \{u : u \geq \xi, \ u \text{ is periodic on } Y\}$ and $\xi : Y \to I\!R$ is a given function referred to as the "obstacle". Loosely speaking, the variational inequality Eq. (11) models an elastic membrane being pushed down onto the obstacle formed by the graph of ξ. Then one anticipates that part of the membrane will be in contact with the obstacle, defining the the coincident set $\Omega_C := \{\mathbf{x} \in Y : \ \phi(\mathbf{x}) = \xi(\mathbf{x})\}$. Under some mild conditions, it can be shown the solution ϕ to Eq. (11) in fact satisfies the overdetermined problem

$$\begin{cases} \Delta\phi = -\Delta\xi\chi_{\Omega_C} + f\chi_{Y\setminus\Omega_C} & \text{on } \ Y, \\ \nabla\nabla\phi = \nabla\nabla\xi & \text{on } \ \Omega_C, \\ \text{periodic boundary conditions} & \text{on } \ \partial Y. \end{cases} \tag{12}$$

If, in particular, one chooses a quadratic obstacle $\xi = -\frac{1-f}{2}(\mathbf{x}-\mathbf{d}_0)\cdot\mathbf{Q}(\mathbf{x}-\mathbf{d}_0)$ with $\mathbf{d}_0$ being the center of the unit cell Y, comparing Eq. (12) with Eq. (9)-Eq. (10) one concludes that the coincident set Ω_C is precisely a periodic E-inclusion. The interested reader is referred to Liu *et al.* (2008) for details of the above existence proof.

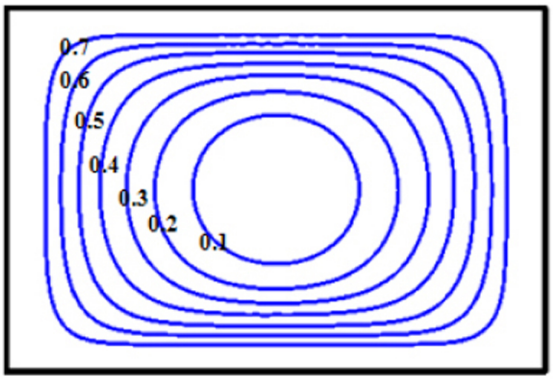

Fig. 2. Periodic E-inclusions (Vigdergauz structures) with unit cell $[0, 1.5] \times [0, 1]$ and isotropic shape matrix $\mathbf{Q} = \mathbf{I}/2$. From inward to outward, the volume fraction of the inclusion increases from 0.1 to 0.7.

Geometrically, the shape of a periodic E-inclusion in $I\!R^n$ is prescribed by the scalar volume fraction f, the symmetric shape matrix $\mathbf{Q} \in I\!R^{n\times n}$ and the unit cell Y associated to the periodicity. In the dilute limit the shape matrix $\mathbf{Q}$ coincides with the *demagnetizaton matrix* of an ellipsoid in the study of ferromagnetics and is determined by the aspect ratios and orientations of the ellipsoid. In two dimensions, explicit parameterizations of periodic E-inclusions are available for a rectangular unit cell (Vigdergauz, 1988; Grabovsky and Kohn, 1995; Liu et al., 2007) and examples of periodic E-inclusions in the unit cell $[0, 1.5] \times [0, 1]$ are shown in Fig. 2 for isotropic shape matrix $\mathbf{Q} = \mathbf{I}/2$ and volume fractions from 0.1 to 0.7. From Fig. 2 we see that a two-dimensional periodic E-inclusion of isotropic shape matrix is roughly a circle at a low volume fraction, say, 0.1, and a rounded rectangle of roughly the same aspect ratio as the unit cell at a high volume fraction, say, 0.7. For more general unit cells and in three dimensions, periodic E-inclusions can be constructed by solving the above variational inequality (11) and numerical calculations show similar qualitative dependence of the shape on the volume fraction (Liu et al., 2007; 2008).

3.2 Applications to magnetoelectric composites

We now solve Eq. (5) by the equivalent inclusion method for periodic E-inclusions. To this end, we first consider the associated *homogeneous* inclusion problem

$$\begin{cases} \nabla \cdot \left[\mathbf{L}^{(m)}\nabla\mathbf{u} + \mathbf{\Sigma}^*\chi_\Omega\right] = 0 & \text{on } Y, \\ \text{periodic boundary conditions} & \text{on } \partial Y, \end{cases} \tag{13}$$

where $\mathbf{\Sigma}^* \in I\!R^{3\times 2}$ is the "eigenstress". We remark that the physical interpretations of equations Eq. (5) and Eq. (13) are different from the classic Eshelby inclusion problem in elasticity, though their forms appear to be the same. Further, the applied periodic boundary conditions in Eq. (5) and Eq. (13) take into account the interactions between the inclusions which are neglected or phenomenologically accounted for by the analysis based on Eshelby's solution.

The solution to Eq. (13) is closely related with the following simple potential problem Eq. (9). To see this, by Fourier transformations we find that

$$\nabla\nabla\phi(\mathbf{x}) = -\sum_{\mathbf{k}\in\mathcal{K}\setminus\{0\}} \frac{\mathbf{k}\otimes\mathbf{k}}{|\mathbf{k}|^2}\hat{\chi}_\Omega(\mathbf{k})\exp(i\mathbf{k}\cdot\mathbf{x}) \qquad \forall\,\mathbf{x}\in Y, \tag{14}$$

where $\mathcal{K}$ is reciprocal lattice associated with the unit cell Y (i.e., Y is a primitive unit cell associated with the lattice $\mathcal{L}$ and $\mathcal{K}$ is the reciprocal lattice of $\mathcal{L}$), and $\hat{\chi}_\Omega(\mathbf{k}) = \int_Y \chi_\Omega \exp(-i\mathbf{k}\cdot\mathbf{x})d\mathbf{x}$ are the Fourier coefficients of the characteristic function $\chi_\Omega(\mathbf{x})$. Similarly, the solution to Eq. (13) can be expressed as

$$\nabla\mathbf{u}\,(\mathbf{x}) = -\sum_{\mathbf{k}\in\mathcal{K}\setminus\{0\}} (\mathbf{N}\boldsymbol{\Sigma}^*\mathbf{k}) \otimes \mathbf{k}\hat{\chi}_\Omega(\mathbf{k}) \exp(i\mathbf{k}\cdot\mathbf{x}), \tag{15}$$

where the 3×3 symmetric matrix $\mathbf{N}(\mathbf{k})$ is the inverse of the matrix $L^{(m)}_{piqj}k_ik_j$. In Eq. (15), for clarity we omit the $\mathbf{k}$-dependence of $\mathbf{N}$ in notation. From the particular form of $\mathbf{L}^{(m)}$ defined in Eq. (4), direct calculations reveal that

$$L^{(m)}_{piqj}k_ik_j = A^{(m)}_{pq}|\mathbf{k}|^2, \qquad \mathbf{N}(\mathbf{k}) = \tfrac{1}{|\mathbf{k}|^2}(\mathbf{A}^{(m)})^{-1}. \tag{16}$$

Comparing Eq. (14) with Eq. (15), we conclude that

$$\nabla\mathbf{u} = (\mathbf{A}^{(m)})^{-1}\boldsymbol{\Sigma}^*\nabla\nabla\phi \qquad \text{on } Y. \tag{17}$$

We emphasize that the above relation between the solution to the system of equations Eq. (13) and the scalar potential problem Eq. (9) holds for any inclusion Ω.

Further, we assume the inclusion Ω is a periodic E-inclusion with shape matrix $\mathbf{Q}$ and volume fraction f. From the definition of periodic E-inclusions discussed above, the solution to Eq. (9) for a periodic E-inclusion satisfies the overdetermined condition Eq. (10). By Eq. (17) and Eq. (10), we conclude that the periodic E-inclusion has the *Eshelby uniformity property* for the homogeneous periodic problem (13) in the sense that the field $\nabla\mathbf{u}$ is uniform inside the inclusion Ω, and is given by

$$\nabla\mathbf{u} = -(1-f)\mathbf{R}\boldsymbol{\Sigma}^* \text{ on } \Omega, \tag{18}$$

where the components of the tensor $\mathbf{R} : I\!R^{3\times 2} \to I\!R^{3\times 2}$ are given by

$$R_{piqj} = \left(\mathbf{A}^{(m)}\right)^{-1}_{pq} Q_{ij} \qquad (p,q = 1,2,3; i,j = 1,2). \tag{19}$$

Here the reader is cautioned that $\nabla\mathbf{u}$ being uniform on periodic E-inclusions for any applied "eigenstress" $\boldsymbol{\Sigma}^*$ depends on a property of tensor $\mathbf{L}^{(m)}$, i.e., the

matrix $\mathbf{N}(\mathbf{k})$ is independent of $\mathbf{k}$ upon being multiplied by a scalar factor $|\mathbf{k}|^2$. From this viewpoint, periodic E-inclusions does not enjoy the full uniformity property as ellipsoids, as shown in Liu (2010) by the complex variable method.

We now consider the inhomogeneous problem (5). Following the equivalent inclusion method we claim that the solution to Eq. (5) is identical to that of Eq. (13) if the average applied field $\mathbf{F}$ for Eq. (5) and the "eigenstress" $\boldsymbol{\Sigma}^*$ for Eq. (13) are related by

$$\triangle\mathbf{L}\mathbf{F} = (1-f)\triangle\mathbf{L}\mathbf{R}\boldsymbol{\Sigma}^* - \boldsymbol{\Sigma}^* = [(1-f)\triangle\mathbf{L}\mathbf{R} - \mathbb{I}]\boldsymbol{\Sigma}^*, \tag{20}$$

where $\triangle\mathbf{L} = \mathbf{L}^{(m)} - \mathbf{L}^{(i)}$, and $\mathbb{I} : I\!R^{3\times 2} \to I\!R^{3\times 2}$ is the identity mapping. To see this, we first notice that a solution to Eq. (13) with uniform field inside Ω (cf. Eq. (18)) satisfies Eq. (5) inside the matrix $Y \setminus \Omega$ since they are the same equations, and inside the inclusion Ω since $\nabla\mathbf{u}$ is uniform on Ω. Further, on the interface $\partial\Omega$ we find that Eq. (5) requires the interfacial conditions

$$[\mathbf{L}^{(i)}(\nabla\mathbf{u}(\mathbf{x}-) + \mathbf{F}) - \mathbf{L}^{(m)}(\nabla\mathbf{u}(\mathbf{x}+) + \mathbf{F})]\mathbf{n} = 0 \qquad \text{on } \partial\Omega, \tag{21}$$

where $\mathbf{n}$ is the outward normal on $\partial\Omega$, and $\mathbf{x}-$ ($\mathbf{x}+$) denotes the boundary value approached from inside (outside) Ω. Similarly, equation (13) implies the interfacial conditions

$$[\mathbf{L}^{(m)}\nabla\mathbf{u}(\mathbf{x}-) + \boldsymbol{\Sigma}^* - \mathbf{L}^{(m)}\nabla\mathbf{u}(\mathbf{x}+)]\mathbf{n} = 0 \qquad \text{on } \partial\Omega. \tag{22}$$

A brief and straightforward algebraic calculation shows that if Eq. (22) is satisfied and $\nabla\mathbf{u}(\mathbf{x}-)$ is given by Eq. (18), then Eq. (21) is satisfied as well for any average applied field $\mathbf{F}$ satisfying Eq. (20). We henceforth conclude that the solution to the homogeneous problem (13) is indeed a solution to the inhomogeneous problem (5) if the uniformity property Eq. (18) holds and the algebraic relation Eq. (20) is satisfied.

To calculate the effective tensor of the composite, by Eq. (7) and Eq. (18) we find that the effective tensor $\mathbf{L}^e$ satisfies

$$\begin{aligned}\mathbf{F}\cdot\mathbf{L}^e\mathbf{F} &= \frac{1}{|Y|}\int_Y \mathbf{F}\cdot\left(\mathbf{L}^{(m)} - \triangle\mathbf{L}\chi_\Omega\right)(\nabla\mathbf{u} + \mathbf{F})\,d\mathbf{x} \\ &= \mathbf{F}\cdot\mathbf{L}^{(m)}\mathbf{F} - f\mathbf{F}\cdot\triangle\mathbf{L}[-(1-f)\mathbf{R}\boldsymbol{\Sigma}^* + \mathbf{F}].\end{aligned}$$

By Eq. (20) we rewrite the above equation as

$$\mathbf{F}\cdot\mathbf{L}^e\mathbf{F} = \mathbf{F}\cdot\mathbf{L}^{(m)}\mathbf{F} + f\mathbf{F}\cdot\boldsymbol{\Sigma}^*.$$

Further, it can be shown that the tensor $(1-f)\triangle\mathbf{LR}-\mathbb{I}$ is invertible for generic cases and the above equation implies

$$\mathbf{L}^e = \mathbf{L}^{(m)} + f[(1-f)\triangle\mathbf{LR}-\mathbb{I}]^{-1}\triangle\mathbf{L}, \tag{23}$$

which is our closed-form formula of the effective properties for two-phase composites of PM and PE materials.

A few remarks are in order regarding Eq. (23). First, it is a rigorous closed-form prediction to the effective properties of periodic composites of PE and PM materials with microstructures being periodic E-inclusions and there is no phenomenological parameters in Eq. (23). Also, we do not need to compute the generalized Eshelby tensor which is usually quite time consuming in the classic analysis based on the Eshelby's works. Second, the assumption of unit cell Y being rectangular is not essential since there exist corresponding periodic E-inclusions for any unit cell with any given positive semi-definite shape matrix $\mathbf{Q}$ with $\mathrm{Tr}(\mathbf{Q}) = 1$ and volume fraction $f \in (0,1)$. If we send the shape matrix $\mathbf{Q}$ to a degenerate matrix with eigenvalues $\{0,\ 1\}$, the inclusion degenerates to a laminate regardless of the unit cell Y and Eq. (23) recovers the formula for simple laminated composites. Third, the anisotropy of the effective tensor $\mathbf{L}^e$ is determined by the anisotropy of microstructure (i.e., the shape matrix $\mathbf{Q}$) and the anisotropy of the materials. As illustrated in Fig. 2, the aspect ratios of the inclusions alone cannot determine the anisotropy of the microstructure (i.e., the shape matrix $\mathbf{Q}$). Another geometric feature, particularly important for periodic composites of any microstructure at high volume fractions, is the unit cell Y or equivalently the inter-distance and inter-orientation between one inclusion and its neighbors. Equation (23) offers a practical and simple way to characterize the anisotropy of the microstructure from the measured anisotropy of one kind of effective properties, e.g., the effective electric conductivity, which in turn can be used to predict other effective properties including the effective ME tensors. Finally, we may use Eq. (23) to design the anisotropy of the microstructure according to the desired anisotropy of the effective ME composites in applications.

4 Applications

Below we apply the closed-form solution Eq. (23) to the design of ME composites. For simplicity we will assume the microstructure is isotropic in the sense that the shape matrix $\mathbf{Q} = \mathbf{I}/2$. A material property of particular interest is the ME voltage coefficient $\alpha_{E,11} = \lambda^e_{11}/\kappa^e_{11}$, where λ^e_{11} (κ^e_{11}) is the effective ME coupling coefficient (dielectric permittivity) of the composite. The effective ME voltage coefficient $\alpha_{E,11}$ relates the overall electric field generated in

Table 1: Material parameters of $BaTiO_3$ [1], $CoFe_2O_4$ [1], P(VDF-TrFE) [2] and Terfenol-D(epoxy) [3,4].

Property	$BaTiO_3$	$CoFe_2O_4$	P(VDF-TrFE)	Terfenol-D(epoxy)
C_{44} (N/m^2)	43.0G	45.3G	0.256G	13.6G
e_{15}(C/m^2)	11.6	0	-0.015	0
q_{15}(N/Am)	0	550	0	108.3
κ_{11}(C$_2$/Nm^2)	11.2×10^{-9}	0.08×10^{-9}	0.07×10^{-9}	0.05×10^{-9}
μ_{11}(Ns^2/C^2)	5×10^{-6}	590×10^{-6}	1.26×10^{-6}	5.4×10^{-6}
λ_{11}(Ns/VC)	0	0	0	0

[1] J. Y. Li, and M. L. Dunn, J. Intell. Mater. Syst. Struct. 9, 404 (1998); [2] Nan, C. W., M. Li, et al., Physical Review B 63(14): 144415 (2001); [3] Y. X. Liu, J. G. Wan, J. -M. Liu, and C. W. Nan, J. Appl. Phys. 94, 5111 (2003); [4] G. Liu, C. -W. Nan, N. Cai, and Y. Lin, J. Appl. Phys. 95, 2660 (2004).

the composite with the applied magnetic field and is the figure of merit for magnetic field sensors.

As a first example, we choose the widely used $BaTiO_3$ (BTO) as the piezoelectric phase and $CoFe_2O_4$ (CFO) as the piezomagnetic phase. Both BTO and CFO are transversely isotropic, i.e. with 6mm symmetry. The independent material constants are listed in Table 1 in Voigt notation, where the xy plane is isotropic and the fiber axis is along the z-direction. Note that in all materials the ME coefficient $\lambda_{11} = 0$. We consider both cases: BTO fibers in a CFO matrix and CFO fibers in a BTO matrix.

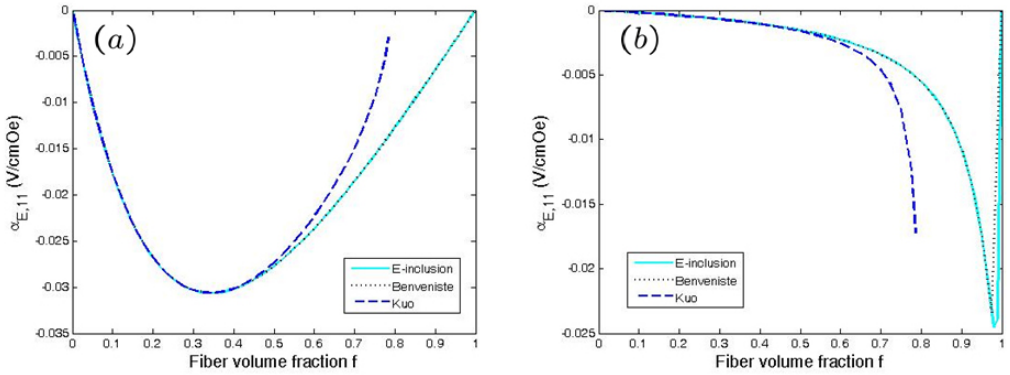

Fig. 3. The predicted ME voltage coefficients versus volume fractions: (a) BTO fibers in CFO matrix and (b) CFO fibers in BTO matrix. In both (a) and (b), the solid line "—" is based on the presented closed-form solution for periodic E-inclusions with shape matrix $\mathbf{Q} = \mathbf{I}/2$, i.e., Eq. (23); the dotted line "..." is from Benveniste (1995); the dashed line "— —" is from Kuo (2011).

Figure 3 shows how the ME voltage coefficient depends on the volume fraction of the inclusion. The ME voltage coefficient is non-zero for every non-zero volume fraction of the inclusion even though this coefficient is zero for each constituent phase. This reflects the magnetoelectric coupling is mediated by the elastic interaction and implies that there is an *optimal* volume fraction for the desired maximum ME voltage coefficient. Figure 3(a) shows the maximum (absolute value) ME voltage coefficient occurs at the volume of $f_{opt} = 0.35$ with $\alpha_{E,11} = 0.0306 V/cmOe$ in the case of BTO fibers in a CFO matrix, whereas Figure 3(b) shows the maximum (absolute value) ME voltage coefficient occurs at the volume of $f_{opt} = 0.98$ with $\alpha_{E,11} = 0.0245 V/cmOe$ in the case of CFO fibers in a BTO matrix. Figures 3(a) & (b) also compare with the effective ME voltage coefficients predicted by Kuo (2011) who used multiple expansion technique and by Benveniste (1995) who employed the composite cylinder assemblage (CCA) model. In Kuo (2011), the curve stops at $f = \pi/4$ when the inclusions begin to touch each other. Still, the overall magnitudes and trends agree well among predictions based on the closed-form solutions for periodic E-inclusions, Kuo's model, and Beveniste's CCA, and in particular Benveniste's CCA gave the same predictions as the present closed-form solutions. Further, our numerical results fulfil the compatibility conditions given in Eq. (21) of the work by Benveniste (1995).

Next, we study how the effective ME voltage coefficient depends on the elastic moduli $C_{44,PE}$ and $C_{44,PM}$, dielectric permittivities $\kappa_{11,PE}$ and $\kappa_{11,PM}$, magnetic permeabilities $\mu_{11,PE}$ and $\mu_{11,PM}$ of the PE and PM materials, piezoelectric coefficient $e_{15,PE}$ of the PE material, and piezomangetic coefficient $q_{15,PM}$ of the PM material. For ease of comparison, we choose the material properties of BTO and CFO as the reference and define the normalized material properties of the PE and PM phases as

$$\hat{C}_{44,PE} = \frac{C_{44,PE}}{C_{44,BTO}}, \quad \hat{C}_{44,PM} = \frac{C_{44,PM}}{C_{44,CFO}}, \quad \hat{\kappa}_{11,PE} = \frac{\kappa_{44,PE}}{\kappa_{44,BTO}},$$

and likewise are $\hat{\kappa}_{11,PM}$, $\hat{\mu}_{11,PE}$, $\hat{\mu}_{11,PM}$, $\hat{e}_{15,PE}$ and $\hat{q}_{15,PM}$. By Eq. (23), we can write the effective voltage coefficient as a function of volume fraction and the normalized material properties of the PE and PM phases

$$\alpha_{E,11} = \alpha_{E,11}(f;\ \hat{C}_{44,PE}, \hat{C}_{44,PM}, \hat{\kappa}_{11,PE}, \cdots). \tag{24}$$

As demonstrated by Fig. 3, there exists an optimal volume fraction f_{opt} for maximum ME voltage coefficients. We can formally write this optimal volume and the corresponding maximum effective ME voltage coefficient as functions of the above normalized properties of the PE and PM phases

$$f_{opt} = f_{opt}(\hat{C}_{44,PE}, \hat{C}_{44,PM}, \hat{\kappa}_{11,PE}, \cdots),$$

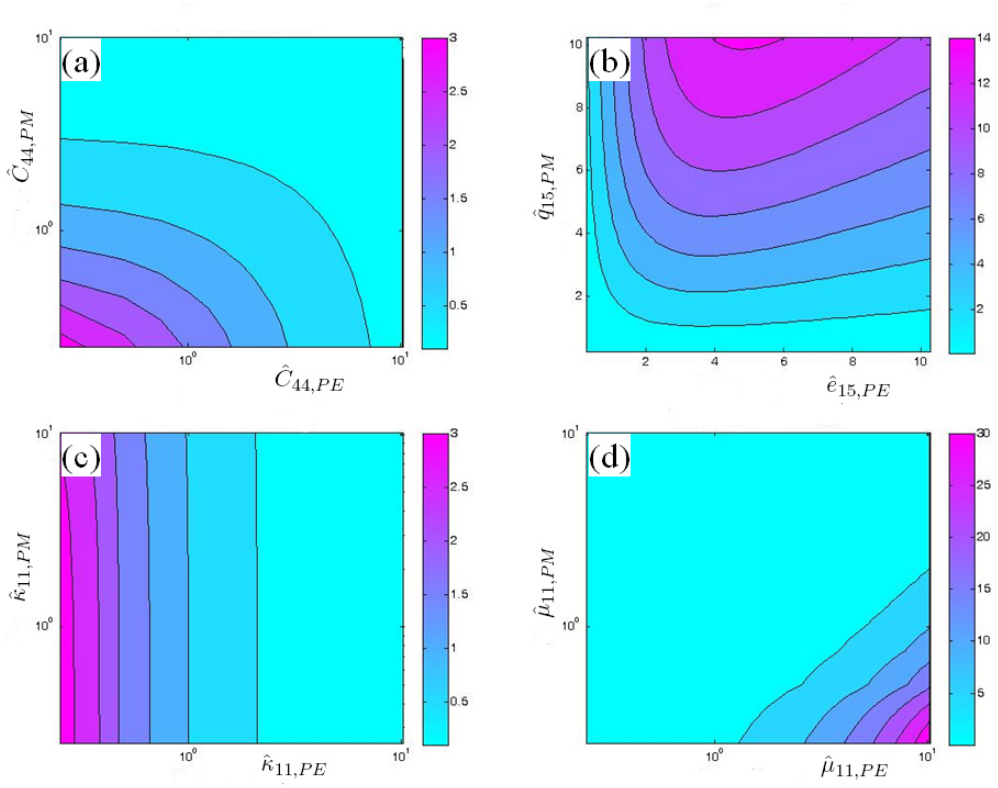

Fig. 4. The contour plots of the maximum effective ME voltage coefficients $\alpha^{\star}_{E,11}$ versus different material parameters for composite of PE fibers in a PM matrix. The unit for ME voltage coefficient is $0.0306V/cmOe$ and the horizontal and vertical axes represent: (a) normalized elastic constants $\hat{C}_{44,PE}$ and $\hat{C}_{44,PM}$; (b) normalized piezoelectric coefficient of PE phase $\hat{e}_{15,PE}$ and normalized piezomagnetic coefficient of PM phase $\hat{q}_{15,PM}$; (c) normalized dielectric permittivities $\hat{\kappa}_{11,PE}$ and $\hat{\kappa}_{11,PM}$; (d) normalized magnetic permeabilities $\hat{\mu}_{11,PE}$ and $\hat{\mu}_{11,PM}$.

$$\alpha^{\star}_{E,11} = \alpha_{E,11}(f_{opt};\ \hat{C}_{44,PE}, \hat{C}_{44,PM}, \hat{\kappa}_{11,PE}, \cdots).$$

Below we numerically compute the maximum ME voltage coefficient $\alpha^{\star}_{E,11}$ by Eq. (23) and its dependence of the normalized material properties of PE and PM phases. These results give important guidelines for practical designs of ME composites of PE and PM materials.

Figure 4 shows the contours of the maximum ME voltage coefficients $\alpha^{\star}_{E,11}$ of PE fibers (over volume fraction f) in a PM matrix at the optimal fibrous volume fraction f_{opt}, where the maximum ME voltage coefficients $\alpha_{E,11,\text{BTO in CFO}} = 0.0306V/cmOe$ of BTO fibers in a CFO matrix is chosen as the unit for the ME voltage coefficient $\alpha^{\star}_{E,11}$ for ease of comparison. The optimal volume fractions of PE phase f_{opt} vary from 0.28 to 0.64, whose exact values can be easily computed by numerically maximizing the effective ME voltage coefficient over $f \in [0, 1]$ (cf. Eq. (24)). In Fig. 4 (a) the horizontal and vertical axes represent the normalized elastic constants of PE and PM phases in logarithmic scale,

respectively. It is observed that the ME voltage coefficient increases when either the fiber or matrix's elastic constant decreases. Therefore, softer PM and PE materials are preferred for improving the ME voltage coefficients of composites of PE fibers in a PM matrix. Figure 4(b) shows the contours of the maximum ME voltage coefficients $\alpha^{\star}_{E,11}$ versus the piezoelectric and piezomagnetic constants in linear scale. For a fixed piezoelectric coefficient e_{15}, the ME voltage coefficient increases monotonically as the piezomagnetic coefficient q_{15} increases. However, for a fixed normalized piezomagnetic coefficient q_{15} and as the piezoelectric coefficient e_{15} increases, the ME voltage coefficient increases first and decreases after certain optimal e_{15}. Therefore, a large piezomagnetic coefficient q_{15} but a nontrivial optimal piezoelectric coefficient e_{15} are preferred for improving the ME voltage coefficients of composites of PE fibers in a PM matrix. Figure 4(c) shows the contours of the maximum ME voltage coefficient $\alpha^{\star}_{E,11}$ versus the normalized electric permittivities of PE and PM phases in logarithmic scale. We observe that smaller PE permittivity $\kappa_{11,PE}$ gives rise to larger ME voltage coefficient. However, the PM permittivity $\kappa_{11,PM}$ does not influence ME effect much. Figure 4(d) shows the contours of the maximum ME voltage coefficient $\alpha^{\star}_{E,11}$ versus the normalized magnetic permeabilities of the PE and PM phases in logarithmic scale. We observe that increasing the PE's magnetic permeability largely enhances the ME voltage coefficient, and on the contrary, increasing the PM's magnetic permeability lowers the ME voltage coefficient. Therefore, a large magnetic permeability of the PE phase and a small magnetic permeability of the PM phase are preferred for improving the ME voltage coefficient for composites of PE fibers in a PM matrix.

We now turn to the case of PM fibers (with isotropic shape matrix $\mathbf{Q} = \mathbf{I}/2$) in a PE matrix. Figure 5 shows the contours of the maximum ME voltage coefficients $\alpha^{\star}_{E,11}$ at the optimal fibrous volume fraction f_{opt}, where the maximum ME voltage coefficients $\alpha_{E,11,\text{CFO in BTO}} = 0.0245V/cmOe$ of CFO fibers in a BTO matrix is chosen as the unit for the ME voltage coefficient for ease of comparison. The optimal volume fractions f_{opt} of PM phase are also computed by numerically maximizing the effective ME voltage coefficient over $f \in [0, 1]$ (cf. Eq. (24)). From Fig. 5(a) we observe that the elastic constant of the PE phase has a much stronger influence on the ME voltage coefficient than that of the PM phase. Again, soft PM and PE phases are preferred for improving the ME voltage coefficient. We also notice that the optimal volume fraction of the PM phase f_{opt} is roughly a constant of 0.98 though the elastic constants of the PM and PE phases change orders of magnitude. From Fig. 5(b) we observe that the ME voltage coefficient increases monotonically as the piezomagnetic coefficient q_{15} of the PM phase increases and there is an optimal piezoelectric coefficient e_{15} of PE phase for maximum ME voltage coefficient of composites of PM fibers in a PE matrix. We also notice that the optimal volume fraction of the inclusion f_{opt} is roughly a constant of 0.98. Figure 5(c) & (d) shows that to improve the ME voltage coefficient of composites of PM fibers in a PE matrix, we shall engineer the PM fibers and PE matrix such that the electric

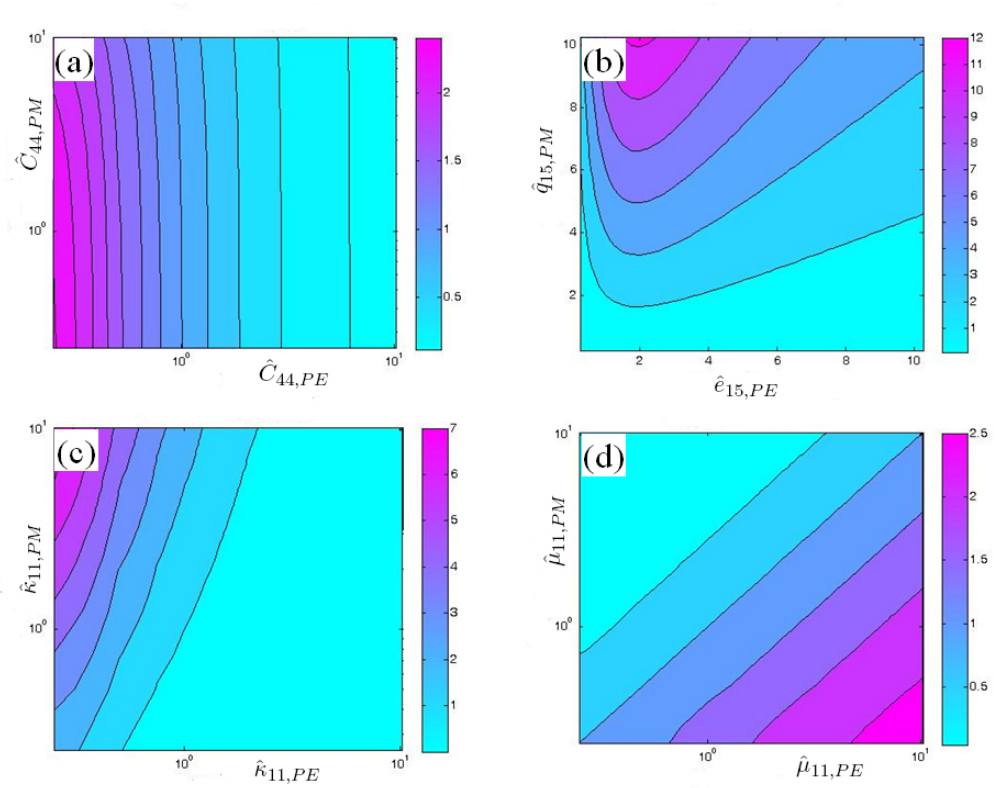

Fig. 5. The contour plots of the maximum effective ME voltage coefficients $\alpha^{\star}_{E,11}$ versus different material parameters for composite of PM fibers in a PE matrix. The unit for ME voltage coefficient is $0.0245V/cmOe$ and the horizontal and vertical axes represent: (a) normalized elastic constants $\hat{C}_{44,PE}$ and $\hat{C}_{44,PM}$; (b) normalized piezoelectric coefficient of PE phase $\hat{e}_{15,PE}$ and normalized piezomagnetic coefficient of PM phase $\hat{q}_{15,PM}$; (c) normalized dielectric permittivities $\hat{\kappa}_{11,PE}$ and $\hat{\kappa}_{11,PM}$; (d) normalized magnetic permeabilities $\hat{\mu}_{11,PE}$ and $\hat{\mu}_{11,PM}$.

permittivity $\kappa_{11,PM}$ of the PM phase is enhanced and the magnetic permeability $\mu_{11,PM}$ is reduced, and on the contrary, the electric permittivity $\kappa_{11,PE}$ of the PE phase is reduced and the magnetic permeability $\mu_{11,PE}$ is enhanced. The optimal volume fraction f_{opt} varies from 0.92 to 0.98 for cases shown in Fig. 5(c) & (d).

Motivated by the above study, we study ME composites of P(VDF-TrFE) and Terfenol-D(epoxy) (TD(epoxy)) since they have much lower elastic constants, electric permittivity, and magnetic permeability. Further, a particulate ME composite made of P(VDF-TrFE) and TD was also studied by Nan et al.(2001a,b) which shows that the flexible composite exhibits markedly larger coupling effect. For P(VDF-TrFE) in a TD(epoxy) matrix, the maximum is attained at volume fraction $f = 0.34$ where ME voltage coefficient $\alpha_{E,11} = 0.1051V/cmOe$ (Figure 6(a)). For TD(epoxy) in a P(VDF-TrFE) matrix, the maximum occurs at the volume fraction $f = 0.87$ where the coupling

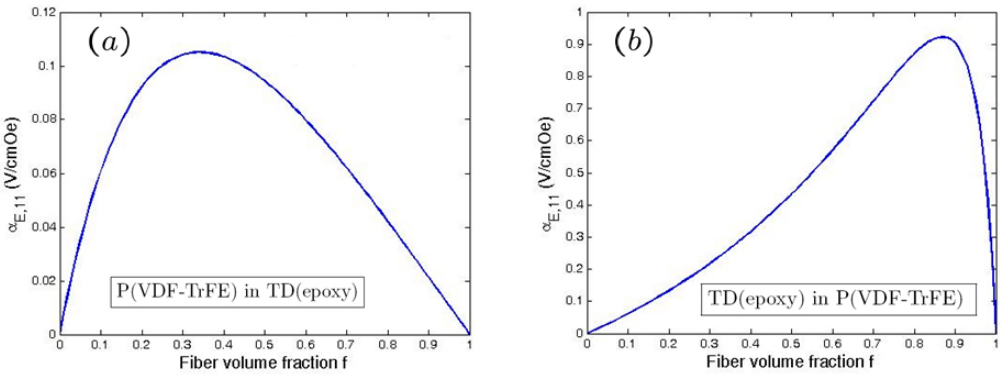

Fig. 6. The predicted ME voltage coefficients. P(VDF-TrFE) is the fiber phase and TD(epoxy) is the matrix phase for (a). TD(epoxy) is the fiber phase and P(VDF-TrFE) is the matrix phase for (b).

effect $\alpha_{E,11} = 0.9221 V/cmOe$ (Figure 6(b)). Both of them are around 3.5 times enhancement of the coupling coefficients compared to their BTO/CFO counterparts.

5 Summary and Discussion

The coexistence of magnetic and electric ordering and their interaction in magnetoelectric (ME) materials have stimulated considerable scientific and technological interest in recent years for potential applications in actuators, sensors and storage devices. By considering a simple model of periodic two-phase composites of piezoelectric (PE) and piezomagnetic (PM) materials, we derive a closed-form solution to the effective properties of the composite in terms of material properties of the constituent phases and simple geometric parameters: the volume fraction f of the fiber phase and the shape matrix $\mathbf{Q}$ which characterizes the anisotropy of the microstructure. The predicted effective properties are realizable by microstructures of periodic E-inclusions.

Based on this closed-form solution, we study the dependence of a particular material property of interest, the ME voltage coefficient, on the volume fraction of the fiber phase and the material properties of the PE and PM phases. In particular, we obtain the following design principles for ME fibrous composites of PE and PM phases:

(1) There exists an optimal volume fraction for maximum ME voltage coefficient which can be obtained by maximizing Eq. (24) over volume fraction $f \in (0, 1)$. This is probably the most important conclusion of our study since the volume fraction is the easiest controllable design parameters.

(2) Softer materials are desirable for improving the ME voltage coefficient.
(3) For composites of PE fibers in a PM matrix and PM fibers in a PE matrix (cf. Figs. 4-5), it is desirable to have larger piezomagnetic coefficient but smaller magnetic permeability in the PM phase, smaller electric permittivity but larger magnetic permeability in the PE phase. Further, there exists an optimal value of the piezoelectric coefficient of the PE fibers for maximum ME voltage coefficient.
(4) The dielectric permittivity of PM phase has a much stronger effect on the ME voltage coefficient for composites of PM fibers in a PE matrix than for composites of PE fibers in a PM matrix (cf. Figs. 4(c) and 5 (c)) and is preferably large.

Acknowledgements

We are grateful to acknowledge the supports under Grant Numbers: NSC 99-2221-E-009-053 (H.-Y. Kuo) and NSF CMMI–1101030 (L. P. Liu). This work was completed while LL held a position at the Department of Mechanical Engineering, University of Houston; the support and hospitality of the department is gratefully acknowledged.

References

Aboudi, J., 2001. Micromechanical analysis of fully coupled electro-magneto-thermo-elastic multiphase composites. Smart Mater. Struct. **10**, 867-877.

Benveniste, Y., 1995. Magnetoelectric effect in fibrous composites with piezoelectric and piezomagnetic phases . Phys. Rev. B **51**, 16424-16427.

Bichurin, M. I., Petrov, V. M., Yu. V. Kiliba, Yu. V., 2002. Magnetic and magnetoelectric susceptibilities of a ferroelectricferromagnetic composite at microwave frequencies. Phys. Rev. B **66**, 134404.

Camacho-Montes, H., Sabina, F. J., Bravo-Castillero, J., Guinovart-Daz, R., Rodrguez-Ramos R., 2009. Magnetoelectric coupling and cross-property connections in a square array of a binary composite. Int. J. Eng. Sci **47**, 294-312.

Eerenstein W., Mathur, N. D., Scott, J. F., 2006. Multiferroic and magnetoelectric materials. Nature **442**, 759-765.

Eshelby, J. D., 1957. The determination of the elastic field of an ellipsoidal inclusion and related problems. Proc. R. Soc. London A **241**, 376-396.

Fennie, C. J., 2008. Ferroelectrically induced weak ferromagnetism by design. Phy. Rev. Lett. **100**, 167203.

Fiebig, M., 2005. Revival of the magnetoelectric effect. J. Phys. D: Appl. Phys. **38**, R123–R152.

Grabovsky, Y., Kohn R.v., 1995. Microstructures minimizing the energy of a two phase composite in two space dimensions (II): The "Vigdergauz microstructure". J. Mech. Phys. Solids **43**, 949–972.

Huang, J. H., 1998. Analytical predictions for the magnetoelectric coupling in piezomagnetic materials reinforced by piezoelectric ellipsoidal inclusions. . Phys. Rev. B **58**, 12-15.

Huang, J. H., Kuo, W. -S., 1997. The analysis of piezoelectric/piezomagnetic composite materials containing ellipsoidal inclusions. J. Appl. Phys. **81**, 1378-1386.

Kimura, T., Goto, T., Shintani, H., Ishizaka, K., Arima T., Tokura, Y., 2003 Magnetic control of ferroelectric polarization. Nature **426** Nov., 55.

Kumar, A., Sharma, G. L., Katiyar, R. S., Pirc, R., Blinc, R., Scott, J. F., 2009. Magnetic control of large room-temperature polarization. J. Phys.: Condens. Matter **21**, 382204.

Kuo, H.-Y., 2011. Multicoated elliptic fibrous composites of piezoelectric and piezomagnetic phases. Int. J. Eng. Sci. **49**, 561-575.

Kuo, H.-Y., Pan, E., 2011. Effective magnetoelectric effect in multicoated circular fibrous multiferroic composites. J. Appl. Phys. **109**, 104901.

Kuo, H.-Y., Slinger, A., Bhattacharya, K., 2010. Optimization of magnetoelectricity in piezoelectricity in piezoelectric-magnetostrictive bilayers. Smart Mater. Struct. **19**, 125010.

Lee, J., Boyd IV, J. G., Lagoudas D. C., 2005. Effective properties of three-phase electro-magneto-elastic composites. Int. J. Eng. Sci. **43**, 790-825.

Li, J. Y., 2000. Magnetoelectroelastic multi-inclusion and inhomogeneity problems and their applications in composite materials . Int. J. Eng. Sci. **38**, 1993-2001.

Li, J. Y., Dunn, M. L., 1998a. Anisotropic coupled-field inclusion and inhomogeneity problems. Philos. Mag. A **77**, 1341-1350.

Li, J. Y., Dunn, M. L., 1998b. Micromechanics of magnetoelectroelastic composite materials: average fields and effective behaviour. J. Intel. Mat. Syst. Struct. **9**, 404-416.

Liu, L. P., 2009. Effective conductivities of two-phase composites with a singular phase.. J. Appl. Phys. **105** 103503.

Liu, L. P., 2010. Solutions to periodic Eshelby inclusion problem in two dimensions.. Math. Mech. Solids. **15** 557–590.

Liu, L. P., James, R. D., Leo, P. H., 2007. Periodic inclusion-matrix microstructures with constant field inclusions. Metal. Mater. Trans. A **38** 781-787.

Liu, L. P., James, R. D., Leo, P. H., 2008. New extremal inclusions and their applications to two-phase composites. Arch. Rational Mech. Anal., Accepted. Preprint available at http://math.rutgers.edu/∼ll502/papers/Einclusions.pdf.

Liu, G, Nan, C.-W., Cai, N., Lin, Y., 2004. Dependence of giant magnetoelectric effect on interfacial bonding for multiferroic laminate composites of rare-earth-iron alloys and lead-zirconate-titanate. J. Appl. Phys. **95** 2660-2664.

Liu, Y. X., Wang, J. G., Nan, C. W., 2003. Numerical modeling of magnetoelecitrceffect in a composite structure. J. Appl. Phys. **94** 5111-5117.

Milton, G. W., 2002. The Theory of Composites, Cambridge University Press.

Mura, T., 1987. Micromechanics of Defects in Solids, Martinus Nijhoff.

Nan, C.-W., 1994. Magnetoelectric effect in composites of piezoelectric and piezomagnetic phases. Phys. Rev. B **50**, 6082-6088.

Nan, C.-W., Bichurin, M. I., Dong, S, Viehland, D., Srinivasan, G., 2008. Multiferroic magnetoelectric composites: Historical perspective, status, and future directions. J. Appl. Phys. **103**, 031101.

Nan, C.-W., Li, M., Feng, X, Yu, S., 2001a. Possible giant magnetoelectric effect of ferromagnetic rare-earth-iron-alloys-filled ferroelectric polymers. Appl. Phys. Lett. **78**, 2527.

Nan, C.-W., Li, M., Huang, J. H., 2001b. Calculations of giant magnetoelectric effects in ferroic composites of rare-earth-iron alloys and ferroelectric polymers. Phys. Rew. B **63**, 144415.

Ni, Y., He, L., Khachaturyan, A. G., 2010. Equivalency principle for magnetoelectroelastic multiferroics with arbitrary microstructure: The phase field approach. J. Appl. Phys. **108**, 023504.

Srinivas, S., Li, J. Y., 2005. The effective magnetoelectric coefficients of polycrystalline multiferroic composites. Acta Mater. **53**, 4135-4142.

Srinivas, S., Li, J. Y., Zhou, Y. C., Soh, A. K., 2006. The effective magnetoelectroelastic moduli of matrix-based multiferroic composites. J. Appl. Phys. **99**, 043905.

Vigdergauz, S. B., 1988. The geometrical characteristics of equally-strong boundaries of elastic bodies. PMM U.S.S.R. **52**, 371–376.

Wu, T. -L., Huang, J. -H., 2000. Closed-form solutions for the magnetoelectric coupling coefficients in fibrous composites with piezoelectric and piezomagnetic phases. Int. J. Solids Struct. **37**, 2981-3009.

Zheng, H., Wang, J., Lofland, S. E., Ma, Z., Mohaddes-Ardabili, L., Zhao, T., Salamanca-Riba, L., Shinde, S. R., Ogale, S. B., Bai, F., Viehland, D., Jia, Y., Schlom, D. G., Wuttig, M., Roytburd, A., Ramesh, R., 2004. Multiferroic $BaTiO_3$-$CoFe_2O_4$ Nanostructures. Science **303** 661-663.